JACS
JOURNAL OF THE AMERICAN CHEMICAL SOCIETY

COMMUNICATION

pubs.acs.org/JACS

Latticelike Smectic Liquid Crystal Phase in a Rigid-Rod Helical Polyisocyanide with Mesogenic Pendants

Takashi Kajitani,[*,†,∥] Hisanari Onouchi,[†] Shin-ichiro Sakurai,[†] Kanji Nagai,[†,‡,⊥] Kento Okoshi,[†] Kiyotaka Onitsuka,[§] and Eiji Yashima[*,†,‡]

[†]Yashima Super-structured Helix Project, Exploratory Research for Advanced Technology (ERATO), Japan Science and Technology Agency (JST), Japan

[‡]Department of Molecular Design and Engineering, Graduate School of Engineering, Nagoya University, Chikusa-ku, Nagoya 464-8603, Japan

[§]Department of Macromolecular Science, Osaka University, 1-1 Machikaneyama-cho, Toyonaka, Osaka 560-0043, Japan

Supporting Information

ABSTRACT: We report a unique macromolecule consisting of a rodlike helical polyisocyanide backbone with a narrow molecular weight distribution and rigid mesogenic chiral pendants linked via a flexible spacer that exhibits lyotropic nematic and latticelike new smectic (*lat*-Sm) liquid crystal phases at different concentrations. The unprecedented *lat*-Sm phase is associated with the smectic ordering of both the stiff polymer backbone and the rigid-rod side groups. A detailed investigation of the films using X-ray scattering and atomic force microscopy revealed a novel tilted smectic layer structure of the polymer backbone aligned perpendicular to the smectic layer of the mesogenic pendants, which arrange in an antiparallel overlapping interdigitated manner.

The investigation of molecular self-assembly and self-organization, resulting in new complex liquid crystal (LC) phases, is among the most fascinating research areas.[1] In particular, since Freiser's prediction[2] and the subsequent discovery of the biaxial nematic (N_b) LC phase (Figure 1A),[3] this emerging topic has attracted significant attention because of its potential device applications with the possibility of much faster switching.[4] Another biaxial phase with an unusual layer structure, namely, the biaxial smectic (SmA_b) phase composed of orthogonally aligned molecules in its layers (Figure 1B), was also discovered.[5] These biaxial phases have been observed not only in small-molecule-based, plate[5c,d] and bent-core "banana-shaped" molecules,[3c−e,5b,5d] but also in polymeric systems consisting of flexible polymers with platelike mesogenic pendants (side-chain LC polymers)[3b,5a] and main-chain LC polymers.[3a] Although the first SmA_b phase was observed in a side-chain LC polymer upon cooling of its N_b phase,[5a] a limited number of unique LC phases are available from synthetic polymers.

On the other hand, biological helical polymers such as DNA form complex LC structures [e.g., a two-dimensional smectic (2D-Sm) phase when DNA is complexed with a cationic liposome in a lyotropic system[6]] originating from their main-chain stiffness with a controlled helical sense. Rodlike helical polymers with inherent chain stiffness (large persistence length) and a narrow molecular weight distribution (MWD) can exhibit a smectic (Sm) LC phase in which the stiff helical polymers self-assemble into a layered structure with a uniform thickness on length scales of tens of nanometers,[7] whereas those with broad MWDs form cholesteric or nematic phases.[8]

It has been considered that stiff main-chain polymers with mesogenic pendants (i.e., combined main-chain and side-chain LC polymers) have the potential to form new phases.[9] However, despite the wealth of phases produced by combining main-chain and side-chain LC polymers, they have received little attention, probably because of the lack of main-chain rigidity and controlled molecular architectures.[10] We now report a class of combined main-chain and side-chain LC polymers represented by poly-**1**, which contains a rodlike helical polyisocyanide with a narrow MWD bearing rigid mesogenic 4-[(*S*)-2-methylbutoxycarbonyl]-biphenyl residues linked via a flexible dodecyl spacer and an (*S*)-alanine (Ala) moiety (Figure 1C). This polymer exhibits a lyotropic nematic LC phase and a new latticelike smectic (*lat*-Sm) LC phase.

Our design approach builds upon our previous findings that similar helical polyisocyanides that bear (*S*)- or (*R*)-Ala residues with long alkyl chains as the pendants and have a controlled molecular length and handedness (right- or left-handed helix) can be prepared by helix-sense-selective living polymerization with an achiral ethynediyl-bridged palladium−platinum (Pd−Pt) complex as the initiator; the resulting polyisocyanides (poly-**2**; Figure 1C) possess an almost perfect one-handed helix and form an Sm LC phase, as directly observed by atomic force microscopy (AFM) and revealed by X-ray diffraction (XRD).[7c] The polyisocyanides possess an unprecedented long persistence length of 220 nm stabilized by intramolecular hydrogen-bonding networks through the neighboring amide N−H groups;[11] this value is the highest among all synthetic helical polymers reported to date and comparable to those of biological, multi-stranded helical polymers such as triple-stranded helical collagen and schizophyllan.[12]

Poly-**1**[13] has a backbone structure and Ala-based pendant subunit identical to those in poly-**2** and shows a similar circular dichroism (CD) spectrum in the main-chain imino chromophore region (Figure 2A). The Cotton effect sign and intensity at

Received: February 5, 2011
Published: May 31, 2011

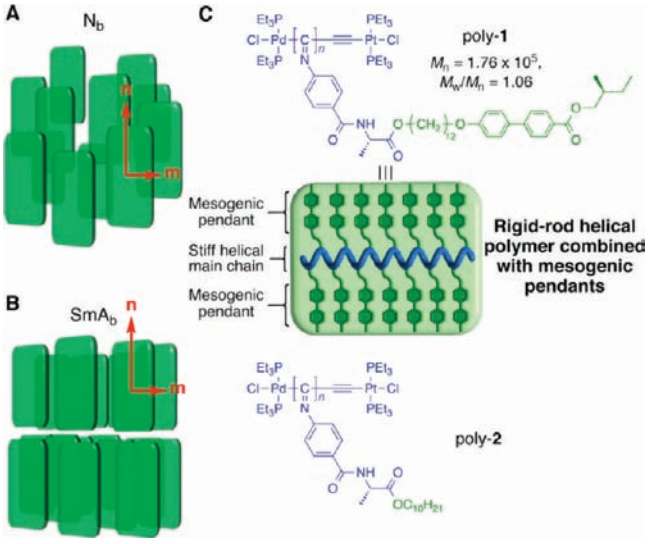

Figure 1. (A, B) Packing structures of platelike molecules in the (A) biaxial nematic (N_b) and (B) biaxial smectic (SmA_b) phases. (C) Structures and schematic illustration of polyisocyanide (poly-**1**) composed of a stiff helical main chain with a controlled helicity (blue) bearing rodlike mesogenic pendants (green). The structure of poly-**2** is also shown.

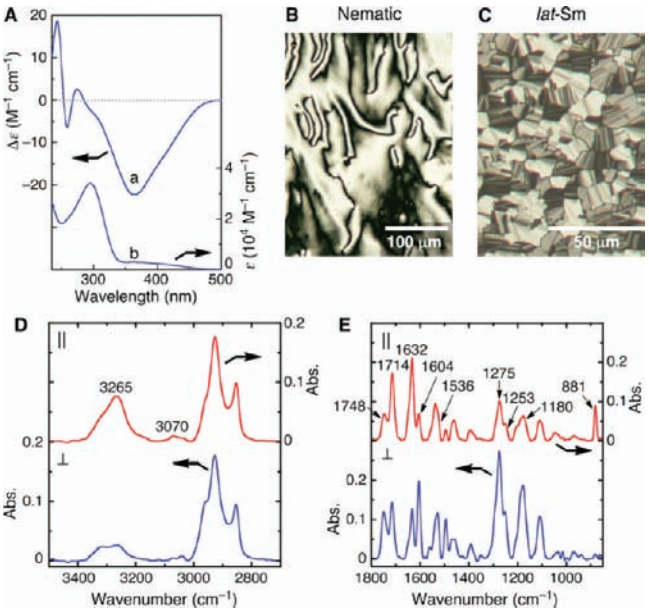

Figure 2. Spectroscopic and optical properties of helical poly-**1**. (A) CD (a) and absorption (b) spectra of poly-**1** in $CHCl_3$ (0.2 mg/mL) at 25 °C. (B, C) Polarized optical micrographs of (B) the schlieren texture of the nematic LC phase and (C) the fanlike texture of the new *lat*-Sm LC phases of poly-**1** in $CHCl_3$. (D, E) Polarized FT-IR spectra of an oriented poly-**1** film with the incident light polarized parallel (||, red) and perpendicular (⊥, blue) to the applied electric field. The film was prepared on a CaF_2 substrate from a concentrated LC toluene solution in an electric field (6000 V/cm).

~360 nm for poly-**1** ($\Delta\varepsilon_{first}$ = −22.2) suggest that the polymer likely possesses an almost perfect left-handed helical structure.[7c]

Polarized optical microscopy of a concentrated solution of poly-**1** in $CHCl_3$ (~15 wt %) demonstrated that the polymer

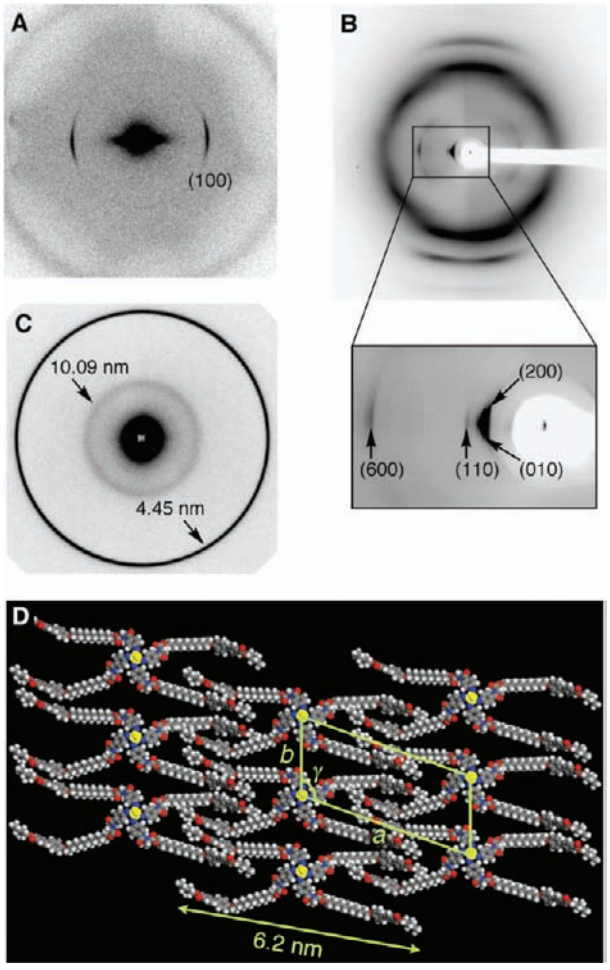

Figure 3. X-ray analyses of poly-**1**. (A) SAXS and (B) WAXD patterns of an oriented poly-**1** film prepared from a concentrated nematic LC benzene solution (~15 wt %). The vertical direction nearly corresponds to the helix axis. The reflections were indexed with a monoclinic lattice (a = 4.90 nm, b = 2.24 nm, c = 1.35 nm, γ = 115°), suggesting a 15/4 helical structure. (C) SR-SAXS pattern of a film of Pd-eliminated, nonoriented poly-**1** ($M_n = 15.9 \times 10^4$) prepared from a concentrated smectic LC $CHCl_3$ solution. The spacing of an inner reflection ($d_{SR\text{-}SAXS}$) was 10.09 nm. (D) Schematic illustration of the proposed packing structure of poly-**1** (tetramer) in the oriented polymer film based on the WAXD and SAXS measurement results. The main-chain carbon atoms are shown in yellow.

forms a nematic phase, as evidenced by its indisputably clear schlieren texture (Figure 2B) that exclusively consists of two-brush disclinations,[5d] which is an important diagnostic for the presence of a biaxial phase; however, we did not have concrete evidence for the biaxial nematic phase rather than a nematic phase at present. An increase in the concentration produced a fan-shaped texture being typical of an Sm LC phase (Figure 2C).[14] Furthermore, this mesomorphic texture was retained after complete removal of the solvent, resulting in a polymer film with the Sm layer structure, as evidenced by its XRD and AFM measurement results (see below).

Polarized IR spectra of an electric-field-induced oriented film of poly-**1** with the incident light polarized parallel (||) and perpendicular (⊥) to the applied electric field (Figure S2)[15] revealed the relative orientations of the helical backbone and the mesogenic pendant groups of the combined polyisocyanide (Figure 2D,E). Sharp signals assigned to the amide NH and

dx.doi.org/10.1021/ja201133d | *J. Am. Chem. Soc.* 2011, 133, 9156–9159

carbonyl stretching (amide I) bands at 3265 and 1632 cm^{-1}, respectively, suggested the formation of intramolecular hydrogen-bonding networks.[7c,11a] The dichroic ratios ($[A_{\parallel}/A_{\perp}]$) for the selected functional groups of poly-**1** (Table S1) indicated that the the polar amide N−H (ν_{NH}) and carbonyl groups (amide I) were arranged parallel to the electric-field applied to the poly-**1** film, resulting in the uniaxial orientation of the rodlike helical backbone parallel to the direction of the applied electric field. On the other hand, the aromatic ester C−O (ν_{C-O}-II) and ether C−O−C (ν_{C-O-C}) groups tended to be oriented perpendicular to the applied electric field (Figure 2E). Thus, the long axes of the mesogenic pendants were likely aligned perpendicular to the helical backbone axis.

Figure 3A,B shows small-angle X-ray scattering (SAXS) and wide-angle X-ray diffraction (WAXD) patterns, respectively, for an oriented poly-**1** film prepared from a concentrated LC benzene solution in an electric field (Figure S2). These revealed apparent meridional and equatorial reflections, leading to a 15/4 helical structure [i.e., a 15 units per 4 turns (15/4) helix][7c] with a monoclinic lattice (parameters: a = 4.90 nm, b = 2.24 nm, c = 1.35 nm, γ = 115°) (Table S2 and Figure 3D). These XRD patterns identified a bilayer-type architecture[9a,16] in which the mesogenic pendants ($l_{pendant}$ = 6.2 nm) are arranged in an antiparallel overlapping interdigitated manner, giving a length difference of 4.45 nm between the polyisocyanide backbone layers.

Synchrotron-radiation SAXS (SR-SAXS) of a poly-**1** film[17] prepared from a concentrated smectic LC $CHCl_3$ solution demonstrated a weak inner reflection with a spacing of 10.09 nm as well as a strong outer reflection of 4.45 nm attributable to the interdigitated lateral packing of the rod polymer (Figure 3C). We also found that the observed inner spacing became shorter (8.70 and 8.50 nm) when lower-molecular-weight poly-**1**s (M_n = 12.7 × 10^4, M_w/M_n = 1.09 and M_n = 12.2 × 10^4, M_w/M_n = 1.10, respectively) were used (Figure S3). Thus, the inner spacing of 10.09 nm corresponds to the smectic layer distance of the polymer backbones.

An AFM image of a Pd-eliminated poly-**1** thick film prepared from a concentrated $CHCl_3$ solution (1.0 mg/mL) on highly oriented pyrolytic graphite (HOPG)[7c,18] clearly revealed a smectic-like self-assembly of the polymer chains with a controlled spacing (Figure 4A). The layer structure was nearly perpendicular to the direction of the polymer main-chain axes. The average layer spacing increased with the increasing M_n of the polymers from 14 to 16 nm (M_n = 12.7 × 10^4 and 15.9 × 10^4, respectively) (Figure 4A and Figure S4B). However, these layer spacings as estimated using AFM were significantly different from those determined using SR-SAXS ($d_{SR\text{-}SAXS} < d_{AFM}$). We then performed AFM measurements on thin films of Pd-eliminated poly-**1** prepared from a dilute benzene solution (0.005 mg/mL) on HOPG, which also showed a 2D-Sm-like assembly of the polymer chains with average layer spacings of 21 and 16 nm (Figure 4B and Figure S4C, respectively). The difference in the layer spacings for the thick and thin films may be due to the difference in the interactions between the polymers and the HOPG substrate. In addition, the average main-chain lengths (L_n) of these polyisocyanides (Figure S5) were indeed longer than the layer spacings determined by SR-SAXS. Thus, we consider that poly-**1** forms a Sm-C-like tilted layer structure in the *lat*-Sm phase.

On the basis of the results presented here, we propose that the polyisocyanides form a platelike structure composed of a rigid helical backbone with the lateral mesogenic pendants oriented perpendicular to the polymer backbone axis. Furthermore, the

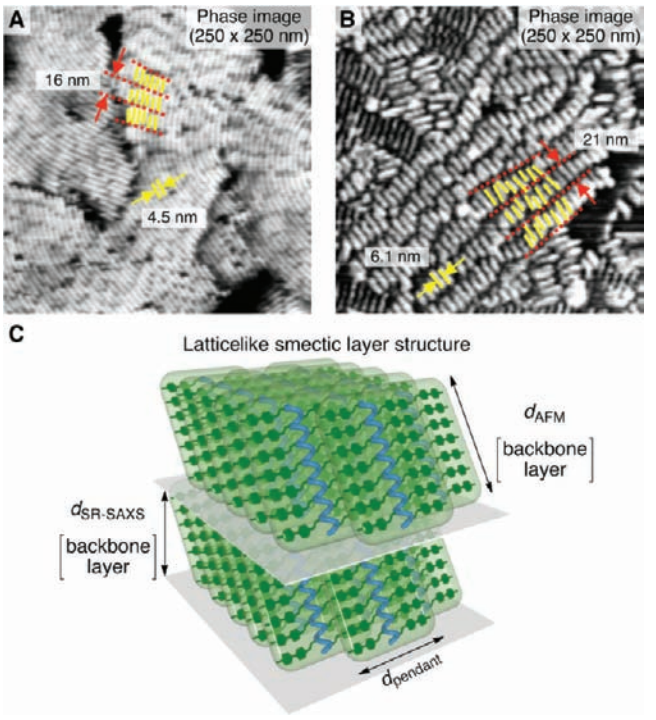

Figure 4. Self-assembled smectic layer structures of poly-**1**. (A, B) AFM phase images of (A) a thick film and (B) self-assembled 2D Pd-eliminated poly-**1** (M_n = 15.9 × 10^4) on HOPG. The yellow bars and red dotted lines indicate the individual polymer chains and 2D smectic layers with respect to the polymer backbone axis, respectively. (C) Schematic illustration of a possible layer structure of poly-**1** in the *lat*-Sm phase.

mesogenic pendants most likely form the bilayer smectic structure in an antiparallel overlapping interdigitated manner. The SR-SAXS and AFM results support the tilted smectic layer structure of the polymer backbones perpendicular to the layer plane of the mesogenic pendants. Consequently, a class of combined main-chain and side-chain LC polymers (i.e., the rodlike helical polyisocyanide poly-**1**) forms the highly ordered latticelike smectic (*lat*-Sm) LC phase in a concentrated LC solution (Figure 4C). This unprecedented phase behavior was generated by careful design of the constituent polymer, which incorporates rodlike mesogenic pendants linked via a flexible spacer to an exceptionally rigid rod helical backbone with a controlled rod length.

In spite of numerous variations and the number of small-molecule-based LC phases, it is difficult for such small molecules to form a complicated latticelike smectic structure because of the size limit. Realization of the *lat*-Sm phase is significant because it opens up the possibility of fabricating new types of liquid-crystalline electro-optical devices. We anticipate that the combined main-chain and side-chain LC polymers may form further unprecedented, complicated packing structures in an LC system because various combinations of smectic structures between the rodlike backbones and the pendant layers are possible. We are currently investigating the interplay between the helical structure and the dynamic behavior of the nematic and *lat*-Sm phases.

■ ASSOCIATED CONTENT

Supporting Information. Full experimental details, FT-IR data, SAXS and WAXD data, and AFM images. This material is available free of charge via the Internet at http://pubs.acs.org.

AUTHOR INFORMATION

Corresponding Author

kajitani@riken.jp; yashima@apchem.nagoya-u.ac.jp

Present Addresses

[‖]Advanced Science Institute, RIKEN, 2-1 Hirosawa, Wako, Saitama 351-0198, Japan.

[⊥]Department of Applied Chemistry, Graduate School of Engineering, Nagoya University, Chikusa-ku, Nagoya 464-8603, Japan.

ACKNOWLEDGMENT

We thank Professors Atsushi Takano and Yushu Matsushita (Nagoya University) for their help with the SR-SAXS measurements. This work was supported in part by a Grant-in-Aid for Scientific Research from the Japan Society for the Promotion of Science (JSPS) and JST. K.N. expresses his thanks for a JSPS Research Fellowship for Young Scientists (6683).

REFERENCES

(1) (a) *Handbook of Liquid Crystals*; Demus, D., Goodby, J., Gray, G. W., Spiess, H. W., Vill, V., Eds.; Wiley-VCH: Weinheim, Germany, 1998. (b) Tschierske, C. *J. Mater. Chem.* **2001**, *11*, 2647–2671. (c) Kato, T.; Mizoshita, N.; Kishimoto, K. *Angew. Chem., Int. Ed.* **2006**, *45*, 38–68. (d) Goodby, J. W.; Saez, I. M.; Cowling, S. J.; Görtz, V.; Draper, M.; Hall, A. W.; Sia, S.; Cosquer, G.; Lee, S.-E.; Raynes, E. P. *Angew. Chem., Int. Ed.* **2008**, *47*, 2754–2787.

(2) Freiser, M. J. *Phys. Rev. Lett.* **1970**, *24*, 1041–1043.

(3) (a) Kricheldorf, H. R.; Domschke, A. *Macromolecules* **1996**, *29*, 1337–1344. (b) Severing, K.; Saalwächter, K. *Phys. Rev. Lett.* **2004**, *92*, No. 125501. (c) Madsen, L. A.; Dingemans, T. J.; Nakata, M.; Samulski, E. T. *Phys. Rev. Lett.* **2004**, *92*, No. 145505. (d) Acharya, B. R.; Primak, A.; Kumar, S. *Phys. Rev. Lett.* **2004**, *92*, No. 145506. (e) Prasad, V.; Kang, S.-W.; Suresh, K. A.; Joshi, L.; Wang, Q.; Kumar, S. *J. Am. Chem. Soc.* **2005**, *127*, 17224–17227.

(4) Luckhurst, G. R. *Thin Solid Films* **2001**, *393*, 40–52.

(5) (a) Leube, H. F.; Finkelmann, H. *Makromol. Chem.* **1991**, *192*, 1317–1328. (b) Pratibha, R.; Madhusudana, N. V.; Sadashiva, B. K. *Science* **2000**, *288*, 2184–2187. (c) Hegmann, T.; Kain, J.; Diele, S.; Pelzl, G.; Tschierske, C. *Angew. Chem., Int. Ed.* **2001**, *40*, 887–890. (d) Yelamaggad, C. V.; Prasad, S. K.; Nair, G. G.; Shashikala, I. S.; Rao, D. S. S.; Lobo, C. V.; Chandrasekhar, S. *Angew. Chem., Int. Ed.* **2004**, *43*, 3429–3432.

(6) Rädler, J. O.; Koltover, I.; Salditt, T.; Safinya, C. R. *Science* **1997**, *275*, 810–814.

(7) (a) Yu, S. M.; Conticello, V. P.; Zhang, G.; Kayser, C.; Fournier, M. J.; Mason, T. L.; Tirrell, D. A. *Nature* **1997**, *389*, 167–170. (b) Okoshi, K.; Kamee, H.; Suzaki, G.; Tokita, M.; Fujiki, M.; Watanabe, J. *Macromolecules* **2002**, *35*, 4556–4559. (c) Onouchi, H.; Okoshi, K.; Kajitani, T.; Sakurai, S.-i.; Nagai, K.; Kumaki, J.; Onitsuka, K.; Yashima, E. *J. Am. Chem. Soc.* **2008**, *130*, 229–236.

(8) (a) Green, M. M.; Peterson, N. C.; Sato, T.; Teramoto, A.; Cook, R.; Lifson, S. *Science* **1995**, *268*, 1860–1866. (b) Cornelissen, J. J. L. M.; Donners, J. J. J. M.; de Gelder, R.; Graswinckel, W. S.; Metselaar, G. A.; Rowan, A. E.; Sommerdijk, N. A. J. M.; Nolte, R. J. M. *Science* **2001**, *293*, 676–680. (c) Watanabe, J.; Kamee, H.; Fujiki, M. *Polym. J.* **2001**, *33*, 495–497. (d) Kim, J.; Novak, B. M.; Waddon, A. J. *Macromolecules* **2004**, *37*, 8286–8292. (e) Nagai, K.; Sakajiri, K.; Maeda, K.; Okoshi, K.; Sato, T.; Yashima, E. *Macromolecules* **2006**, *39*, 5371–5380. (f) Okoshi, K.; Sakurai, S.-i.; Ohsawa, S.; Kuniaki, J.; Yashima, E. *Angew. Chem., Int. Ed.* **2006**, *45*, 8173–8176. (g) Liu, J.; Lam, J. W. Y.; Tang, B. Z. *Chem. Rev.* **2009**, *109*, 5799–5867. (h) Nagai, K.; Okoshi, K.; Sakurai, S.-i.; Banno, M.; Azam, A. K. M. F.; Kamigaito, M.; Okamoto, Y.; Yashima, E. *Macromolecules* **2010**, *43*, 7386–7390.

(9) (a) Watanabe, J.; Tominaga, T. *Macromolecules* **1993**, *26*, 4032–4036. (b) Zhang, J. J.; Ge, A.; McCreight, K. W.; Ho, R.-M.; Wang, S.-Y.; Jin, X.; Harris, F. W.; Cheng, S. Z. D. *Macromolecules* **1997**, *30*, 6498–6506.

(10) (a) Schaefer, K. E.; Keller, P.; Deming, T. J. *Macromolecules* **2006**, *39*, 19–22. (b) Chen, X.-F.; Shen, Z.; Wan, X.-H.; Fan, X.-H.; Chen, E.-Q.; Ma, Y.; Zhou, Q.-F. *Chem. Soc. Rev.* **2010**, *39*, 3072–3101.

(11) (a) Okoshi, K.; Nagai, K.; Kajitani, T.; Sakurai, S.-i.; Yashima, E. *Macromolecules* **2008**, *41*, 7752–7754. For helical polyisocyanopeptides stabilized by intramolecular hydrogen bonds, see ref 8b and:(b) Cornelissen, J. J. L. M.; Rowan, A. E.; Nolte, R. J. M.; Sommerdijk, N. A. J. M. *Chem. Rev.* **2001**, *101*, 4039–4070.

(12) Sato, T.; Teramoto, A. *Adv. Polym. Sci.* **1996**, *126*, 85–161.

(13) Left-handed helical poly-**1** was prepared by living polymerization of the corresponding monomer with the Pd−Pt catalyst in tetrahydrofuran (THF) at 55 °C for 20 h (Scheme S1), which produced both perfectly right- and left-handed helical polyisocyanides with different molecular weights and sufficiently narrow MWDs. The left-handed helical poly-**1** was easily fractionated with acetone as an acetone-insoluble fraction and used in the present study; the number-average molecular weight (M_n) and its distribution (M_w/M_n) were 1.76×10^5 and 1.06, respectively, as determined by size-exclusion chromatography (SEC) in THF containing 0.1 wt % tetra-*n*-butylammonium bromide (TBAB) as the eluent with standard polystyrenes. (Figure S1).

(14) Dierking, I. *Textures of Liquid Crystals*; Wiley-VCH: Weinheim, Germany, 2003.

(15) Okoshi, K.; Kajitani, T.; Nagai, K.; Yashima, E. *Macromolecules* **2008**, *41*, 258–261.

(16) Schenning, A. P. H. J.; Fransen, M.; Meijer, E. W. *Macromol. Rapid Commun.* **2002**, *23*, 265–270.

(17) Poly-**1** was treated with CuCl in piperidine to eliminate the terminal Pd residues, and the resulting Pd-eliminated poly-**1** was fractionated using preparative SEC ($M_n = 1.59 \times 10^5$, $M_w/M_n = 1.07$) prior to the SR-SAXS measurements (Scheme S2).[7c]

(18) (a) Sakurai, S.-i.; Okoshi, K.; Kumaki, J.; Yashima, E. *Angew. Chem., Int. Ed.* **2006**, *45*, 1245–1248. (b) Kumaki, J.; Sakurai, S.-i.; Yashima, E. *Chem. Soc. Rev.* **2009**, *38*, 737–746.